CardioVascular and Interventional Radiology

Cardiovasc Intervent Radiol (2000) 23:47–54

LABORATORY INVESTIGATION

Mechanical Properties of Metallic Stents: How Do These Properties Influence the Choice of Stent for Specific Lesions?

John F. Dyet, William G. Watts, Duncan F. Ettles, Anthony A. Nicholson

Department of Radiology, Royal Hull Hospitals NHS Trust, Hull Royal Infirmary, Anlaby Road, Hull HU3 2JZ, UK

Abstract

Purpose: To assess selected balloon-expandable and self-expanding stents for radial force, flexibility, radio-opacity, and trackability, and to relate these physical characteristics to potential indications for placement.

Methods: Force–strain curves were plotted for each stent and the force required to produce 50% luminal narrowing was recorded. The ability of the stent to show elastic recoil following deformation was also noted. Flexibility was measured by bending the stents against a force transducer and recording the force required per degree of flexion. Radio-opacity was measured by comparing each stent against a standard aluminum step wedge. Trackability was measured by testing the ability of the stent on its delivery system to track over angles of 90° and 60°.

Results: The balloon-expandable stents showed greater radial strength and radio-opacity but, apart from the AVE Iliac Bridge stent, showed poorer flexibility and trackability. The self-expanding stents showed less radial force but were able to re-expand following deformity. They were generally more flexible and had better trackability but lower radio-opacity.

Conclusion: There is no stent which exhibits all the ideal properties required and therefore the interventionist will need to keep a range of stents available if all lesions are to be addressed.

Key words: Stents, metallic—Mechanical properties—Radial force—Flexibility—Radio-opacity—Trackability

Over the last few years there has been a great increase in the number of commercially available endovascular stents. There are now in excess of 40 different stents available for use in the coronary circulation and more than 20 for use in peripheral arteries. For the interventional radiologist this amounts to a bewildering choice of devices, with each manufacturer claiming specific advantages for their stent over its competitors. Independent comparative analysis of stents in vitro has previously been carried out mainly with regard to the radial strength of the earlier generation of endovascular stents [1–3]. This study looked at the physical characteristics of the newer generation of endovascular stents. It is not intended to be a criticism or endorsement of any particular stent, but illustrates how the physical properties of different types of stents might influence operator choice for use in specific lesions in peripheral arteries.

Correspondence to: Dr. J.F. Dyet

Materials and Methods

In order to carry out this assessment, seven of the newer generation of endovascular stents were included for study. Three balloon-expandable and four self-expanding stents were assessed. The balloon-expandable stents were the Palmaz Crown (Johnson & Johnson, Warren, NJ, USA), Iliac Bridge (AVE, Santa Rosa, CA, USA), and VIP (Medtronic, Minneapolis, MN, USA), and the self-expanding stents were the Easy Wallstent (Schneider, Bülach, Switzerland), Memotherm (Bard, Galway, Ireland), Symphony (Boston Scientific, Paris, France) and Instent Vascucoil (Medtronic). For standardization of testing, all stents were of 8-mm diameter and 40-mm length.

The three balloon-expandable stents are manufactured from stainless steel 316L, the Wallstent from elgiloy (an alloy of cobalt and chromium) and tantalum, and the other three from nitinol (named after its place of discovery; Nickel–Titanium Naval Ordinance Laboratory). Nitinol is a thermal memory alloy which can be heat-treated to assume a predetermined shape at a set temperature, which in this case is 30°C. The Wallstent relies on its method of braided construction and the crossing angle of its wires for its self-expanding characteristics.

The stents were assessed for: (1) radial strength, (2) flexibility, (3) radio-opacity, and (4) trackability.

Radial Strength

The force in newtons required to produce a 50% reduction in stent diameter (strain) was determined using the method previously

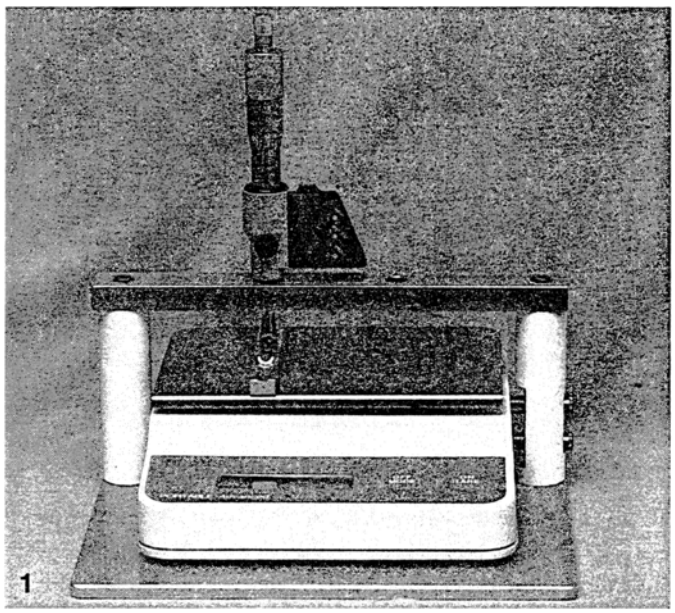

Fig. 1. Balance and micrometer showing a stent in position for measurement.

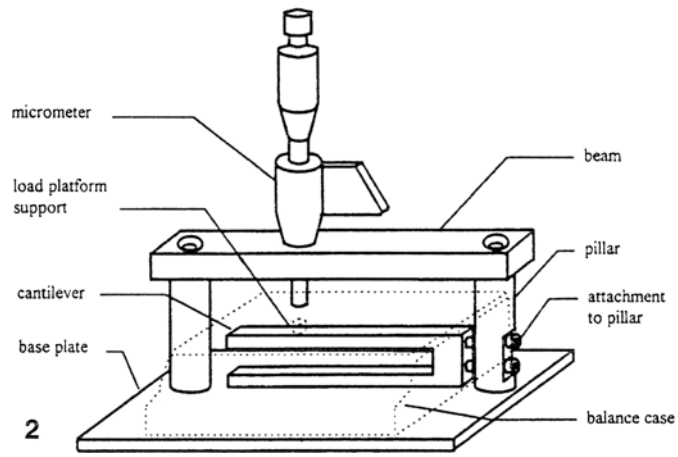

Fig. 2. Diagram of the balance showing the method of securing the cantilever.

described by Lossef et al. [1]. Although Lossef et al. reported the stress/strain relationship, the term "stress" (force/unit area) has not been used here as the contact area between the micrometer head and stent changes as the stent is compressed. The equipment used (Fig. 1) was a digital balance (model CT 1200, Ohaus, Florham Park, NJ, USA) with an accuracy of ±0.3 g of the absolute value, and a range of 0–1200 g. This was calibrated using standard weights, namely the Humberside Authorities Calibration Test Centre weights (Humberside Authorities' Calibration Test Centre, Hull, UK).

The micrometer head (model 350 711-30, Mitutogo, Kawasaki, Japan) had a diameter of 6.35 mm, readability of 0.001 mm, and accuracy of ±2 μm. All stent measurements were undertaken inside an incubator at a steady temperature of 37°C to insure that the nitinol stents in particular were within their optimal operating conditions.

Technical Method and Considerations

The micrometer was secured to a beam, above the balance, supported by two pillars attached to a base plate (Fig. 2). The balance works on the principle of a bending cantilever, so that as the weight on the platform increased, the cantilever deflection increased. This deflection is measured and interpreted as the mass on the balance platform. The load platform on the balance was supported near the end of the cantilever and away from the center line.

These two factors did not affect the performance of the balance when measuring weights. However, as we were interested in the strain applied to the stent from a fixed datum (that is the beam supporting the micrometer), to obtain the true applied strain the cantilever's deflection would have to be subtracted from the apparent stent deformation, indicated by the micrometer reading. This could be expected to be a linear relationship, but the cantilever support, to the side of the balance's plastic case, introduced an additional creep (the deflection continues to change under a constant applied load) and hysteresis (the deflection due to the applied load varies according to whether this is during the increasing or decreasing part of the cycle) to this deflection. To minimize the creep and hysteresis the cantilever was secured to one of the pillars through the case, and the micrometer acted directly above the load platform support on the cantilever (Fig. 2).

Having minimized the creep and hysteresis, the deflection of the balance was then calibrated. The balance was taken through three return runs of increasing the load in increments of 0.005 mm up to a mass reading of over 1000 g.

Data Collection

The micrometer and balance were connected to a personal computer and data points were selectively input into a data logging program, written in Microsoft Visual Basic. This program included an auto-scaling graph-plotting routine which allowed the data to be visualized as it was collected. Also included were a visual indication of the point at which preselected strains were reached (allowing for the balance deflection), the ability to zero the scales and to collect only stable or unstable data—that is data once the balance reading varies less than one decimal point during a fixed time (stable) or data before the balance has settled (unstable). In practice all tests collected only stable data.

Data collected were transferred to a program using Microsoft Excel which adjusted the raw data to allow for the balance deflection, and converted the balance's reading of mass into units of force. A graph was then automatically plotted of force versus strain. The stents were supported in shallow troughs and clamped to the trough at each end (Fig. 3). The troughs were of 4-mm radius and 1 mm deep. This method was used in an attempt to emulate the status in vivo where the stent, on implantation, is partially constrained but can also shorten and expand to a certain extent. The stents were then compressed using the micrometer head. Each stent was compressed by increasing the projection of the micrometer head in increments of 0.1 mm until a loss of 4 mm of the stent's diameter had been achieved. The projection was decreased in the same steps until the balance reading returned to 0 g. At each incremental step the readings of the balance and micrometer were input into the data logging program.

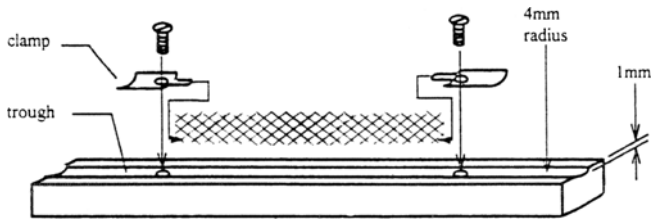

Fig. 3. Diagram showing how the stent is clamped into the trough.

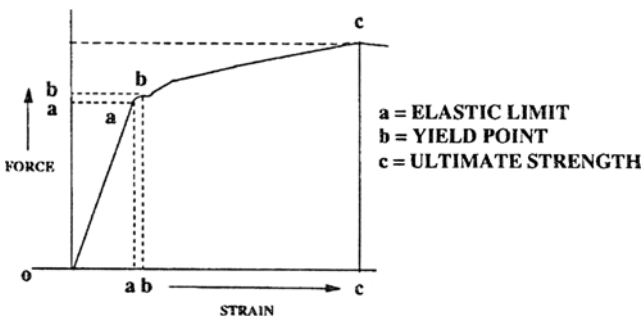

Fig. 4. Standard stress–strain curve for a stainless steel rod.

A typical force–strain curve for stainless steel is shown in Fig. 4. Two types of deformity are demonstrated. The points from 0 to *a* are a straight line and represent "elastic deformation." At any point between 0 and *a* if the force is removed the strain will return to zero, i.e., the metal will revert to its original shape [4]. The line from *b* to *c* shows a curve with a reducing amount of force being required to produce increasing strain. The stainless steel is now exhibiting "plastic deformation" and removal of the force will no longer result in the strain returning to zero, the material being permanently deformed. The point *b* on the curve at which "elastic deformation" becomes "plastic deformation" is known as the "elastic limit." The "yield point" is a point on the force–strain curve at which there is an increase in strain without a corresponding magnitude of increase in force. In the force–strain curves used in this paper the "elastic limit" and "yield point" are effectively synonymous. The gradient of the straight portion of the line is used to calculate Young's modulus of elasticity—the lower the modulus the more elastic the material. Stress–strain diagrams are usually produced when applying tension to a single element of material (i.e., a bar or rod of uniform cross-sectional area), whereas with stents a complex structure is being compressed. Although the structures are uniform and symmetric they are composed of sections that are repeated along the axis. The reaction of the structure to compression will vary depending on the point along a section at which the compression is applied, the length of the sections compared with the diameter of the pressure pad, and at which point this is along its path.

Therefore the terms normally used in tensile testing perhaps do not fully apply, and force–strain curves will only be repeatable to within limited accuracy, but the following can be determined: (1) the order of magnitude of the force with which the stent will resist at a known deformation, (2) whether the stent can be expected to return to its original dimensions when the force has been removed (i.e., whether it is acting elastically), (3) how the force–strain relationship changes as the strain is increased (i.e., whether as the compression increases the stent starts to become less resistive, or vice versa).

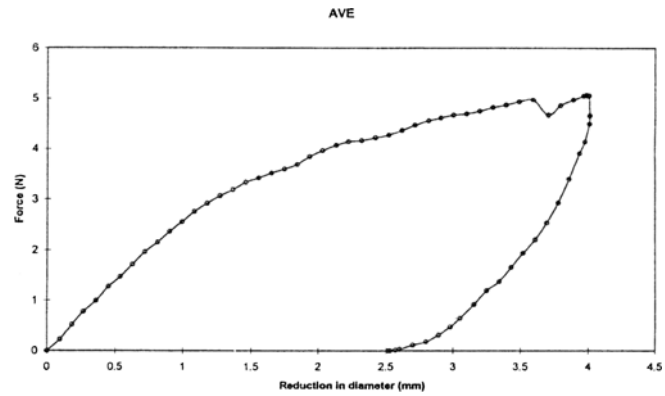

Fig. 5. Force–strain curve for the AVE Iliac Bridge stent.

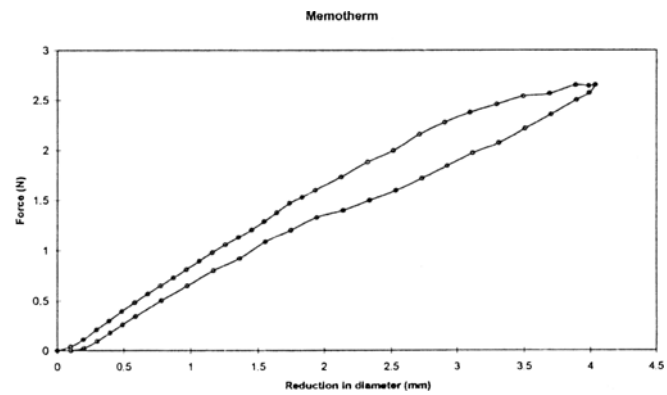

Fig. 6. Force–strain curve for the Memotherm nitinol stent.

Initial elastic deformity is demonstrated in Fig. 5 (AVE stent), where a given increase in force results in a uniform increase in strain, producing a straight line. Once a certain force is reached, however (the yield point), the line begins to curve and plastic deformation begins to take place. As the strain increases the changes in resisting force gradually decrease, producing a fairly smooth collapse. At a strain of 0.5 (50% of the diameter), the resisting force is 5 N. When the applied force is released the stent does not return to its original dimensions, being left at less than 70% of its original diameter.

In Fig. 6 (Memotherm stent) there is a near linear relationship between resisting force and strain, producing elastic deformation. At 0.5 strain (reduction of diameter to 50%), the resisting force is 2.65 N. As the force is released, the stent returns close to its original dimensions, although the relationship is not perfectly elastic.

Flexibility

A measure of the flexibility (or conversely stiffness) of a bar when being bent along its axis can be seen as the ease with which it yields (or is reluctant to yield) to the applied bending forces. Thus, by recording the force with which it tries to maintain its original shape an objective measure of flexibility is obtained.

The device used to measure flexibility of stents during bending was based on a small manual reduction gearbox with a ratio of 198:1. By securing one end of the stent to the output shaft, so the stent was mounted radially, it could then be made to sweep slowly through an arc when the input shaft was turned, with fine angular control achieved through the gearbox. By resisting the movement of

the outer end of the stent with a static force transducer the resistance of the stent to bending could be recorded. The stent was mounted on the shaft by sliding it over a 10-mm-long cylindrical post. The length of stent being flexed was 20 mm.

A back plate secured to the gearbox output shaft face was used to support a mechanical protractor so that the angle through which the stent was flexed could be indicated using a pointer attached to the crank. The force transducer was controlled by a proprietary signal conditioning unit which showed the force output in grams on an alpha-numeric display. The flexing experiments were carried out in an incubator at a temperature of 37°C.

We initially intended to make measurements up to 30° of flexion, but preliminary testing indicated that the more rigid stents (Palmaz and VIP) showed kinking and deformity before this angle and progressively rode up the mounting post; therefore measurements were taken at 10° of flexing. The AVE stent, Wallstent, and Instent Vascucoil, however, could all be flexed to 45° without deformity (the AVE stent in one plane only). All the self-expanding stents resumed their normal shape upon removal of the flexing force. The AVE stent remained in its flexed position but could be returned to its original shape by application of a similar force at 180° to the flexing force.

Radio-opacity

To assess stent radio-opacity it was determined how much aluminum was required to render the stent nonvisible on fluoroscopy. An aluminum step wedge was secured in position under an image intensifier which was centered over it at a fixed height. The diaphragms in the intensifier were adjusted to cover the step wedge precisely. No further adjustment or movement was then allowed. At a set 60 kV and 0.5 mA, each stent was randomly moved up and down on the step of the wedge, and three observers, who were unaware of the position the stent had been placed in, indicated at which levels they could not see the stent. (In addition, some observations were taken with no stent on the step wedge.) The lowest point on the step wedge at which all observers agreed they could not visualize the stent was taken to be the radio-opacity equivalent in millimeters of aluminum.

Trackability

The purpose of the trackability test was to assess the ability of the stent on its delivery system to cross an iliac bifurcation. A model of the iliac bifurcation (Fig. 7) which could be adjusted to provide bifurcation angles from 90° to 60° was used. An 8 Fr flexible sheath of length 45 cm (Arrow, Reading, PA, USA) was positioned over the bifurcation and then each stent on its delivery system was advanced over an Amplatz stiff wire (Boston Scientific). The ability to track over bifurcation angles of 90° and 60° was then measured.

Results

Radial Strength

Table 1 lists the resisting force in newtons at a strain of 0.5 (50% of the original diameter) for each of the stents tested, and the final strain following release of compression. The stents are all of nominal diameter 8 mm. However, in practice this varied slightly and therefore in the force–strain curves the end point is when the stent diameter was reduced by 4 mm. This is given as a strain of 0.5 but this may not be absolutely so. The three balloon-expandable stents showed similar types of curves, as did the four self-expanding stents. The balloon-expandable stents showed plastic deformation with a high resistance to deformity but once deformed remained so, whereas the self-expanding stents show less radial strength but demonstrated elastic deformation and re-expanded on removal of the deforming force.

Flexibility

Table 2 shows the force in grams required to flex each stent to 10°. The lower the force the more flexible the stent.

Radio-opacity

Table 3 shows the amount of aluminum in millimeters required to render each stent nonvisible. The higher the value the more radio-opaque the stent.

Trackability

Table 4 lists stent trackability at 60° and 90° bifurcation angles.

Summarized findings for each stent type tested are given below:

Palmaz Crown

The Palmaz stent has a high radial force (Fig. 8) of 5.3 N at a strain of 0.5 and good radio-opacity (27.5 mm Al) but poor flexibility (flexing force = 148×10^{-2} N at 10°) and poor trackability. It is thus good for calcified and fibrotic lesions. As with all balloon-expandable stents it can be placed accurately. Because of its poor flexibility and trackability it should not be used in tortuous vessels or where normal bends have to be negotiated. Because it exhibits plastic deformity on compression, it should not be used where an external force may be exerted (i.e., over joints).

AVE Iliac Bridge

The AVE stent also has high radial force (Fig. 5) of 5.0 N at a strain of 0.5, good radio-opacity (27.5 mm Al) and shows flexibility (flexing force of 10×10^{-2} N at 10°), although this is in one plane only. In practice the stent rotates as it is introduced and this allows it to follow curves. This stent is again good in calcified and fibrotic lesions; it can be placed accurately and can be used in tortuous vessels. Its deformation, however, is plastic and it should therefore not be used over joints, etc.

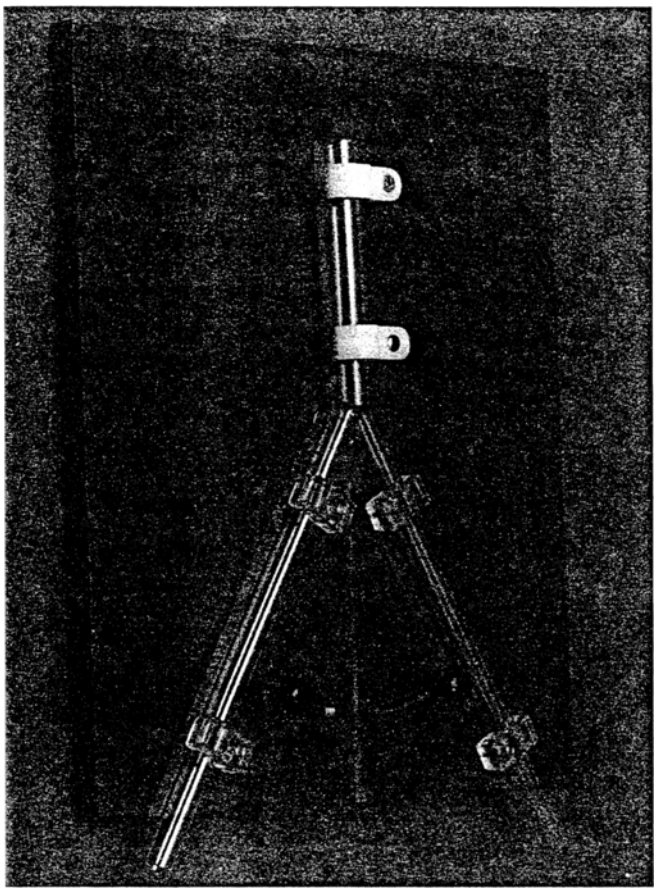

Fig. 7. Model of the aorto-iliac bifurcation used to assess trackability.

Table 1. Radial strength

Stent	Radial strength (N)	Final strain	Deformity
VIP	5.4	0.4	Plastic
Palmaz Crown	5.3	0.39	Plastic
Ave Iliac Bridge	5.0	0.32	Plastic
Wallstent	3.9	0.04	Elastic
Instent Vascucoil	2.7	0.01	Elastic
Symphony	3.4	0.01	Elastic
Memotherm	2.7	0.01	Elastic

Table 2. Flexibility

Stent	Flexibility[a]
Palmaz Crown	148×10^{-2}
VIP	64×10^{-2}
Symphony	49×10^{-2}
Memotherm	20×10^{-2}
Ave Iliac Bridge	10×10^{-2}
Wallstent	3×10^{-2}
Instent Vascucoil	0.5×10^{-2}

[a]Force in newtons required to produce 10° of flexion. The higher the force the less flexible the stent

Table 3. Radio-opacity

Stent	Radio-opacity (mm Al)
Palmaz Crown	27.5
Ave Iliac Bridge	27.5
VIP	27.5
Instent Vascucoil	27.5
Wallstent	25
Memotherm	22.5
Symphony	15

Table 4. Trackability

Stent	Trackability[a]	
	90°	60°
VIP	+	−
Palmaz Crown	−	−
Ave Iliac Bridge	+	+
Wallstent	+	+
Instent Vascucoil	+	+
Symphony	+	+
Memotherm	+	−

[a]The ability of each stent on its delivery system to track over an aortic bifurcation of varying angles

Schneider Wallstent

The Wallstent differs from all the other stents tested in that it relies for its self-expansion on its construction and the fact that it shortens as it expands. Because of this we ran two radial strength tests. The first, with the stent damped at its ends (as it would be following endothelialization), showed a radial strength of 3.9 N at a strain of 0.5 (Fig. 9). The second test was with the stent unconstrained and able to lengthen and shorten freely (as it would immediately on insertion). This showed a radial strength of only 1.8 N at a stress of 0.5 (Fig. 10). The initial radial strength is therefore low, but does increase as the stent becomes fixed in the vessel. It has good flexibility (3×10^{-2} N at 10° flexion) and moderate radio-opacity (25 mm Al). Its trackability is good and the above characteristics make it ideal for tortuous lesions.

Symphony Stent

The radial strength of the Symphony stent is only moderate at 3.4 N at 0.5 strain (Fig. 11), its flexibility is moderate (49×10^{-2} at 10°) and its radio-opacity is low (15 mm Al). It does, however, show good trackability. This stent is suitable for stenoses and short occlusions, and where external force may be applied, as its deformity is elastic.

Memotherm Stent

The radial strength of the Memotherm stent was the lowest of those tested at 2.7 N at 0.5 strain (Fig. 6). It has moderate flexibility (20×10^{-2} at 10°) and radio-opacity (22.5 mm Al). Its trackability is reduced due to a rather rigid delivery system. It can be used for most lesions where a high radial force is not required.

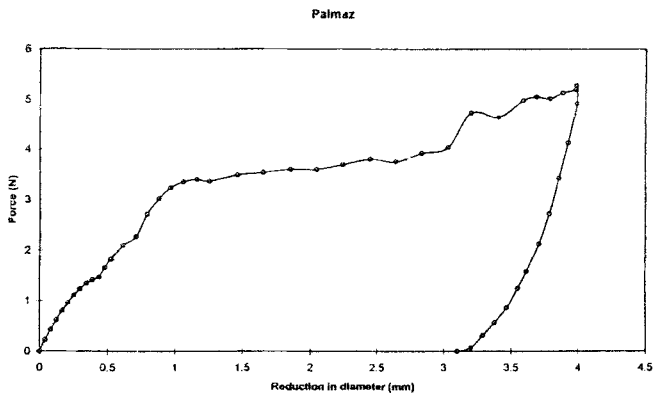

Fig. 8. Force–strain curve for the Palmaz stent.

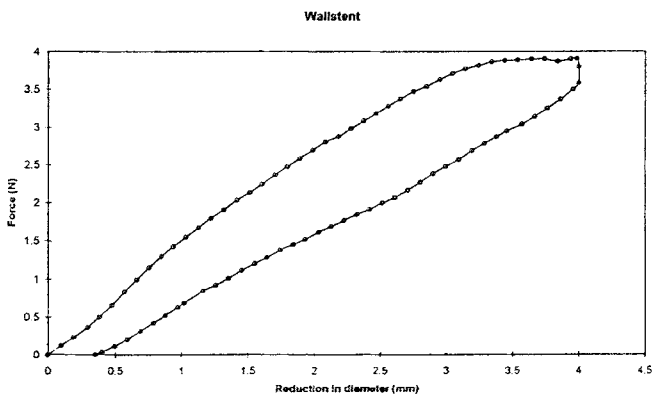

Fig. 9. Force–strain curve for the Wallstent, clamped at both ends.

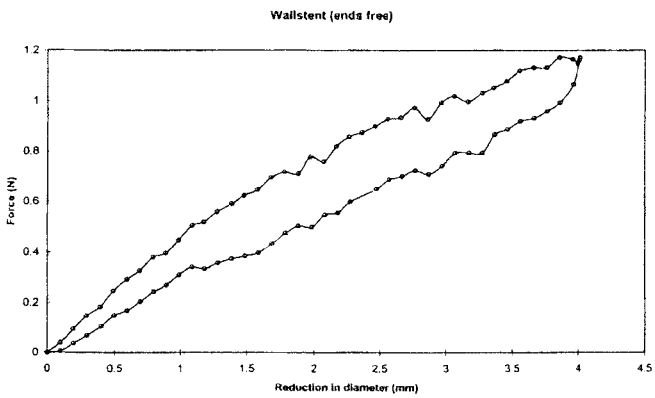

Fig. 10. Force–strain curve for the Wallstent, loose at both ends.

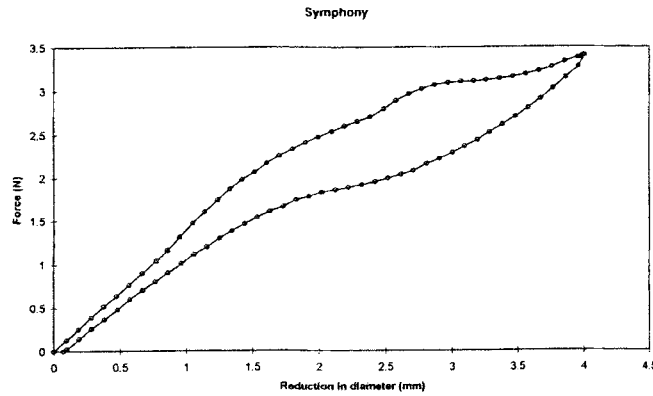

Fig. 11. Force–strain curve for the Symphony stent.

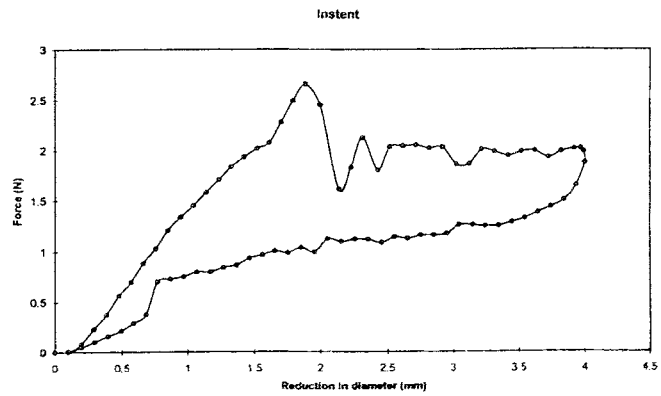

Fig. 12. Force–strain curve for the Instent Vascucoil.

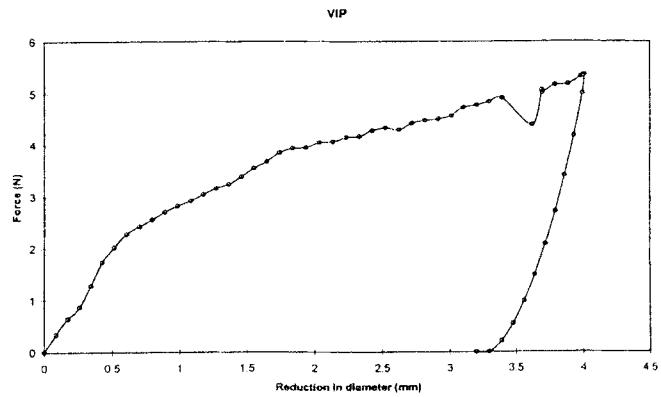

Fig. 13. Force–strain curve for the VIP stent.

Instent Vascucoil

The Instent Vascucoil has a different method of construction, being a simple spring of nitinol wire (Fig. 12). It was difficult to test for radial force as the coils slipped sideways as compression was applied. Fig. 12 shows its stress–strain curve—the highest radial force being taken at 2.7 N at 0.5 strain (Fig. 12 is the best curve we obtained out of many tests).

It has good radio-opacity (27.5 mm Al), excellent flexibility (0.5×10^{-2} N at 10°) and excellent trackability. This stent is now the subject of a randomized trial in the superficial femoral artery. Being the most flexible stent it is probably the best for placing across a joint if required.

VIP Stent

The VIP stent is very similar to the Palmaz Crown stent, with a radial strength of 5.4 N at 0.5 strain (Fig. 13). It is, however, more flexible (64×10^{-2} N at 10°). It has the same indications.

Discussion

For a metallic stent to perform its function adequately (i.e., to provide adequate support) it has to be easy to deploy, conform to the vessel wall, and, once in place, be resistant to dislodgement. To fulfill these requirements, either the force at which the yield point occurs in the force–strain curve should be high or the modulus of elasticity (Young's modulus) should be low.

The stainless steel balloon-expandable stents have a moderately high yield point and high radial force, but with a Young's modulus of 200 GPa they rely on the stent construction rather than the metal for their characteristics.

Nitinol stents, in contrast, depend on the thermal memory effect of the metal itself for their self-expanding properties. Nitinol is an alloy of nickel and titanium, containing 54%–60% nickel by weight. The crystalline structure of the alloy is such that a change in temperature induces a reversible change in that crystalline structure (martensitic transformation), so that it exists in a different form at higher temperature (austenite form) [5]. By adjusting the nickel-to-titanium ratio, and by a form of high-temperature heat treatment, it is possible to predetermine the temperature at which the martensitic transformation occurs (30°C in vitro). At low temperature in its martensite state the metal is flexible and malleable and so can easily be loaded into an introducer system. At the austenite temperature the stent, once released, will expand to its predetermined size and become more rigid. There is a further property of nitinol known as superelasticity [6, 7]. This occurs when a force is applied to the metal in its austenite form (high temperature). The force causes an unstable transformation to the martensitic state and the metal will thus deform. Release of the force causes an immediate reversal to the austenite and more rigid form. The stent in this instance will have re-expanded but not due to a temperature change. Because of these properties nitinol has a low Young's modulus (100 GPa). Thus stent construction does not play such a significant role in its physical characteristics.

The Wallstent, although self-expanding, relies heavily on its method of construction rather than its metallic properties for its characteristics. Figure 9 shows the force–strain curve. There is an apparent elastic limit after which the curve reaches a plateau. On the release of force the stent shows a semi-elastic type of response to return almost to its original shape. The response of the Wallstent to the force is to reduce its diameter by attempting to elongate, and this tends to maintain its circular cross-sectional shape [2], whilst other stents tended to adopt an oval shape on compression. On release of force the stent responds by shortening. The behavior of the Wallstent can be modified by changing the crossing angles of the wires. By reducing the angle from 140° to 120° a less shortening version is produced but at the expense of radial force, although an attempt has been made to maintain the radial strength by increasing the number of wires from 24 to 30. However, Lossef et al. [1] noted that where Wallstents overlapped their radial force was increased by almost a factor of 2.

Fig. 14. The Instent Vascucoil.

Our testing thus demonstrates two distinct groups of stents: those relying on their construction for their inherent properties and those which rely on the metal from which they are manufactured.

The balloon-expandable stents tested are pressured into shape by an angioplasty balloon, and the stent struts are fixed and immobile, giving high radial strength. Flueckiger et al. [3] point out that with such stents the force required to deform them must be greater than that which was used to balloon-expand them. In practice, such forces are only generated if the stent is deployed over a joint or is subjected to a severe external force such as a blow.

The self-expanding stents need little force to deploy them. Once deployed, if the stent is deformed by the lesion, balloon dilatation may improve the result. However, despite obtaining complete expansion with a balloon, if the deforming force of the lesion is greater than the radial force of the stent, deformation of the stent will again occur when the balloon is deflated, although this may be a gradual process. In such cases consideration should be given to implanting a second stent within the first. In addition, the Wallstent has been shown to exhibit decreased radial force if it loses contact with the vessel wall [3], which will compound the effect.

Due to their inelasticity, the balloon-expandable stents should not be used in areas where repeated flexing of the artery occurs. Because of their flexibility and elasticity the Wallstent and Vascucoil are best for this indication, but further work needs to be undertaken to assess metal fatigue levels, as incidents have been reported of stents breaking up when submitted to repeated flexing.

It might be inferred that because the Memotherm stent has a similar construction to the Palmaz stent (i.e., a slotted tube becoming diamonds on expansion) [8], that it would have the advantage of both construction and metallic properties. However, the superelasticity of nitinol, with its transformation from the rigid to the flexible state by pressure, means that this apparent mechanical advantage is lost. In fact, the radial force of this stent is virtually the same as for the Vascucoil, which is made from a single piece of wire in the form of a coiled spring (Fig. 14).

Clearly the major limitation of this study is that all of the foregoing stent evaluation relates to in vitro assessment. While this may give a reasonable indication of how the stents may behave in vivo, there is no good quantitative evidence as to the intrinsic and extrinsic forces that the stent may be subjected to by either the vessel itself or the surrounding tissues. In addition, once a stent becomes endothelialized and incorporated into the vessel wall its characteristics may alter.

We consider that an ideal stent would show the following properties: (1) high radial strength, (2) high radio-opacity, (3) elasticity, (4) flexibility, (5) good trackability. None of the stents tested met all these criteria. The interventionalist will therefore need to have at least one type of balloon-expandable and one type of self-expanding stent available in the department and perhaps other alternatives depending on the complexity of cases undertaken. The search for the perfect stent continues and until this is achieved there will remain a plethora of different stents in the market place.

Acknowledgment. The authors would like to thank Miss C. Whatling for all her help in preparing this manuscript.

References

1. Lossef S, Lutz R, Mundorf J, Barth K (1994) Comparison of mechanical deformation properties of metallic stents with use of stress–strain analysis. J Vasc Interv Radiol 5:341–349
2. Berry JL, Newman VS, Ferrario CM, Routh WD, Dean RH (1996) A method to evaluate the elastic behaviour of vascular stents. J Vasc Interv Radiol 7:381–385
3. Flueckiger F, Sternthal H, Klem GE, Aschauer M, Szolar D, Kleinhappl G (1994) Strength, elasticity and plasticity of expandable metal stents: In vitro studies with three types of stress. J Vasc Interv Radiol 5:745–750
4. Oberg E, Jones FD, Horton HL (1984) Strength of materials. In: Ryffel HH (ed) Machinery's Hand Book, 22nd revised edn. Industrial Press, New York, pp 240–241
5. Gotman I (1997) Characteristics of metals used in implants. J Endourol 11:383–389
6. Shabalovskaya SA (1996) On the nature of the biocompatibility and on medical applications of N_iT_i shape, memory and superelastic alloys. Biomed Mater Eng 6:267–289
7. Ryhanen J, Niemi E, Serlo W, Niemela E, Sandvik P, Pernu H, Salo T (1997) Biocompatibility of nickel-titanium shape memory metal and its corrosion behaviour in human cell cultures. J Biomed Mater Res 35: 451–457
8. Palmaz JC, Windeler SA, Garcia F, Tio F, Sibbitt RR, Reuter S (1986) Atherosclerotic rabbit aortas: Expandible intraluminal grafting. Radiology 160:723–726